

Mesenchymal stem cells improve small intestinal integrity through regulation of endogenous epithelial cell homeostasis

A Sémont^{*1}, M Mouiseddine¹, A François¹, C Demarquay¹, N Mathieu¹, A Chapel¹, A Saché¹, D Thierry¹, P Laloi¹ and P Gourmelon¹

Patients who undergo pelvic or abdominal radiotherapy may develop acute and/or chronic side effects resulting from gastrointestinal tract (GIT) alterations. In this study, we address the question of the regenerative capability of mesenchymal stem cells (MSC) after radiation-induced GIT injury. We also propose cellular targets of MSC therapy. We report that the infusion of human bone marrow-derived MSC (hMSC) provides a therapeutic benefit to NOD/SCID mice undergoing radiation-induced GIT failure. We observed that hMSC treatment brings about fast recovery of the small intestine (structure and function) in mice with reversible alterations and extends the life of mice with irreversible GIT disorders. The effects of hMSC are a consequence of their ability to improve the renewal capability of small intestinal epithelium. hMSC treatment favors the re-establishment of cellular homeostasis by both increasing endogenous proliferation processes (Ki67 immunostaining) and inhibiting apoptosis (TUNEL staining) of radiation-induced small intestinal epithelial cells. Our results suggest that MSC infusion may be used as a therapeutic treatment to limit radiation-induced GIT damage.

Cell Death and Differentiation (2010) 17, 952–961; doi:10.1038/cdd.2009.187; published online 18 December 2009

Radiation exposure during radiotherapy is a mainstay of abdominopelvic malignancy treatments. The efficacy of abdominal or pelvic radiotherapy requires an optimal compromise between normal tissue damage and tumor control, that is the risk/benefit ratio.¹ Intra-abdominal organs located close to cancers can be affected during radiotherapy. The most radiosensitive organ of the intra-abdominal area is the small intestine.² Small intestinal mucosa is composed of a simple columnar epithelium that is folded to form crypts of Lieberkühn (residence site of intestinal stem cells) as well as villi (composed of differentiated epithelial cells). Epithelium has a very fast renewal potential arising from the high level of stem cell proliferation ability. Differentiation of proliferating stem cells around the villus is accompanied by the development of specific functions by epithelial cells, such as nutrient absorption, water and electrolyte transport, mucus secretion, neuropeptide production and immune defense. The preservation of stem cell integrity takes on a crucial importance for the renewal of small intestine epithelium and hence its functionality. Exposure of small intestinal tissue to ionizing radiation may lead to the loss of its integrity by a dose-dependent stem cell depletion initiating gastrointestinal disorders.³ Radiotherapy is associated with a high incidence of undesirable acute and/or chronic gastrointestinal complications that can affect the patient's quality of life and/or may be life threatening.⁴ The severity of acute radiation enteritis may be predictive of more severe chronic gastrointestinal symptoms.⁴ Acute or

chronic side effects can also be aggravated after a radiotherapy accident such as an overdose.⁵ Treatments usually applied to manage acute enteritis are only symptomatic. The lack of curative treatment at present and the potential severity of the disorder highlight the importance of novel and effective therapeutic strategies for gastrointestinal complications after radiation exposure.

Stem cell-based approaches using mesenchymal stem cells (MSC) are promising for the development of future therapy. MSC are currently among the most advanced cell therapy tools, with the availability of three FDA-approved products, Prochymal, Provacel and Chondrogen. MSC treatment has already been used in clinical protocols as an adjunct to bone marrow (BM) transplantation. Clinical studies have reported a possible beneficial therapeutic effect of MSC in supporting the engraftment of hematopoietic stem cells in hematological malignancies,⁶ for the improvement of bone growth by bone matrix synthesis in osteogenesis imperfecta,⁷ and for the reduction of gastrointestinal disorders in patients with severe resistant graft-versus-host disease (GVHD).⁸ Other clinical studies have reported effects of MSC on gastrointestinal healing such as the reversion of colon peritonitis in patients with GVHD⁹ or the treatment of rectovaginal and perianal fistulas in patients with Crohn's disease.¹⁰ In the work reported here, the capability of MSC to induce a therapeutic benefit was analyzed in an experimental model using NOD/SCID mice with radiation-induced small

¹DRPH/SRBE/LRTE, Institut de Radioprotection et de Sûreté Nucléaire, BP no 17, Fontenay aux Roses cedex F-92262, France

*Corresponding author: A Sémont, DRPH/SRBE/LRTE, Institut de Radioprotection et de Sûreté Nucléaire, BP no 17, Fontenay aux Roses cedex F-92262, France. Tel: +33 1 58 35 95 33; Fax: +33 1 58 35 84 67; E-mail: Alexandra.semont@irsn.fr

Keywords: MSC; small intestinal epithelium; recovery; irradiation; apoptosis; proliferation

Abbreviations: BM, bone marrow; EFS, electrical field stimulation; F, human skin fibroblasts; IA, irradiated animals; I_{sc} , Short-circuit current; GIT, gastrointestinal tract; GVHD, graft-versus-host disease; MSC, mesenchymal stem cells; SEU, ulcerated epithelium surface; TBI, total body irradiation

Received 21.4.09; revised 12.10.09; accepted 14.10.09; Edited by R de Maria; published online 18.12.09

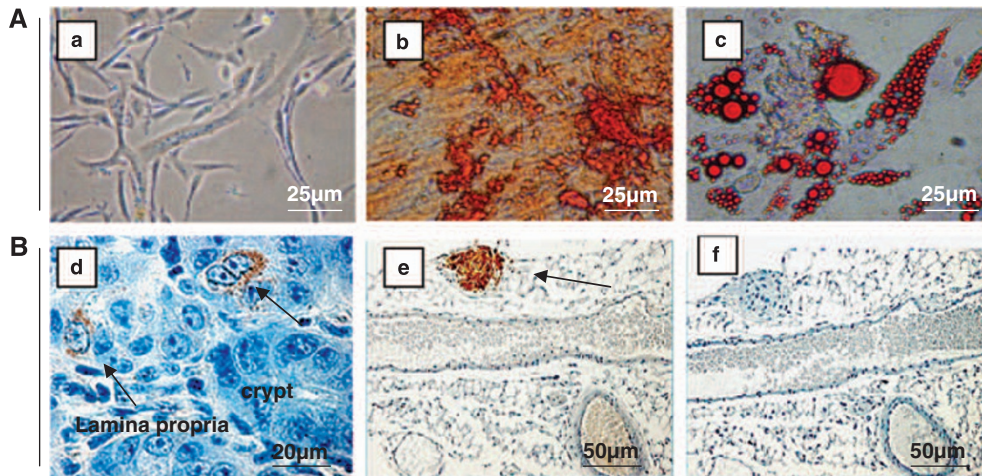


Figure 1 *In vitro* and *in vivo* human bone marrow-derived mesenchymal stem cell (hMSC) properties: (A) *In vitro* multiple differentiation potential of hMSC. Section (a) represents hMSC. After one passage, confluent cells were stained with Alizarin (b) or Oil-Red (c) after 21 days incubation with osteogenic or adipogenic differentiation medium, respectively. Micrographs (original magnification $\times 400$) represent results of 1 of 10 independent experiments. Scale bars $25 \mu\text{m}$. (B) *In vivo* localization of human cells in the small intestine 3 days after irradiation (8.5 Gy). Sections were stained with polyclonal rabbit anti-human β -2-microglobulin antibody (d, e). Specificity of immunohistochemical staining was demonstrated by the absence of staining products using a corresponding non-immune rabbit immunoglobulin, IgG isotypic control (f). Original magnifications $\times 400$ or $\times 600$ corresponding to scale bars 50 and $20 \mu\text{m}$, respectively

intestinal damage. In this experimental model, we analyzed *in vivo* the potential of MSC treatment on cellular mechanisms of cell function restoration.

Results

Multipotential property of human BM-derived MSC. We verified the stem character of human BM-derived MSCs (hMSC) *in vitro* by their ability to carry out multiple differentiations. We used specific induction media to induce osteogenic and adipogenic differentiation of BM-derived cells. As shown in Figure 1A, we found evidence for both osteogenic and adipogenic differentiation potential of the purified hMSC used in this study. Osteogenic differentiation is associated with extracellular precipitate stained with alizarin and corresponding to calcium deposits (Figure 1Ab). Adipogenic differentiation is accompanied by the accumulation of lipid droplets stained by Oil-Red (Figure 1Ac).

Human MSC infusion restores small intestinal integrity. In this part of the study, mice were exposed to a sub-lethal dose of abdominal irradiation (8.5 Gy). Twenty-four hours after irradiation, mice received in the lateral tail vein a total of 5×10^6 hMSC. In this experimental model, the therapeutic benefit of hMSC treatment on radiation-induced small intestinal integrity (structure and function) alterations was tested. We also analyzed cellular mechanisms of hMSC action.

Level of hMSC engraftment. Quantitative PCR analyses indicate a very low frequency of human cell engraftment in the small intestinal epithelium of mice ($0.13 \pm 0.06\%$ corresponding to 0.13 ± 0.06 human MSC engrafted per 1000 mice intestinal cells) 3 days after irradiation. This

engraftment was observed in only 4 of 10 tested animals (A Sémont, unpublished observation). Histological studies of the four positive mice showed that individual human cells homed in to sites in the lamina propria around small intestinal epithelium crypts (Figure 1Bd). Clustered cells were also observed in the mesentery in all (10) tested animals (Figure 1Be).

Functional studies. To obtain evidence for functional integrity of the small intestinal epithelium, we tested two parameters: the secretory response and the absorptive response of epithelial cells. The secretory response was studied by stimulated *in vitro* electrolyte transport measurement and the absorptive response by membrane Na^+/K^+ -ATPase activity evaluation.

Electrolyte transport analysis. Small intestines were mounted in diffusion chambers and voltage clamped after challenge with electrical field stimulation (EFS) (Figure 2a). Exposure of intestinal segments to EFS leads to a transient increase of the short-circuit current (I_{sc}), corresponding to an enhancement of the serosal to mucosal chloride flux. In the control group, the maximum I_{sc} response recorded after EFS exposure was $66.7 \pm 5.7 \mu\text{A}/\text{cm}^2$. Three days after irradiation (irradiated animals (IA) group), the maximal I_{sc} response was significantly reduced, falling to $25.8 \pm 5.8 \mu\text{A}/\text{cm}^2$. Three days after radiation exposure, the observed response to EFS was close to the baseline ($43.9 \pm 5.3 \mu\text{A}/\text{cm}^2$) in the MSC-treated group (IA + MSC group). We tested the specificity of hMSC effects by administering equal numbers of human skin fibroblasts. The injection of fibroblasts showed any adverse radiation effects on the hyporesponsiveness to EFS (IA + F group).

Na^+/K^+ -ATPase activity analysis. Activation of the membrane Na^+/K^+ -ATPase pump is associated with an increase of nutrient absorption across the small intestinal epithelium (Figure 2b). In the control group, the measured

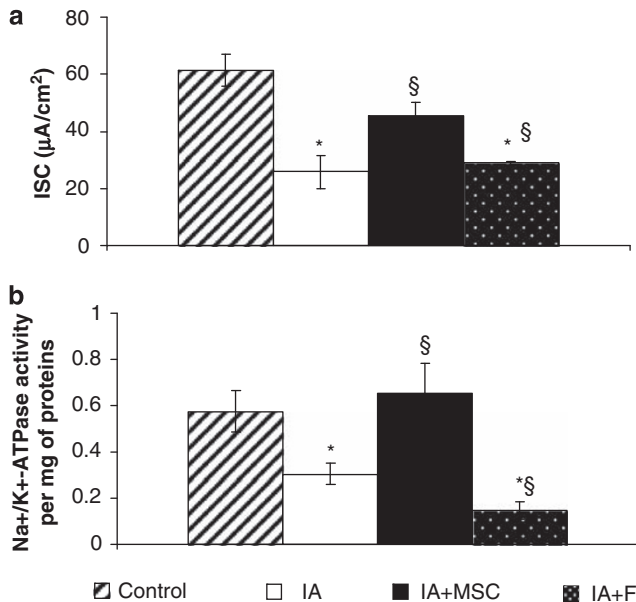


Figure 2 Human bone marrow-derived mesenchymal stem cell (hMSC) infusion restores small intestinal functionality 3 days after irradiation (8.5 Gy): (a) Electrolyte transport was measured by short-circuit current analysis (I_{sc}) after electrical stimulation (5 Hz). Histogram represents the I_{sc} measured per cm^2 of tissue. (b) Membrane Na^+/K^+ -ATPase activity. Histogram represents the enzyme activity measured per mg of protein. Histograms show: control animals, irradiated animals (IA), irradiated animals receiving human MSC injection (IA+MSC) and irradiated animals receiving human skin fibroblast injection (IA+F). Each value represents the average of 24 measurements from two independent experiments (12 animals per experiment). Error bars represent S.E.M. * $P \leq 0.05$ versus control, $\S P \leq 0.05$ versus IA

basal level of Na^+/K^+ -ATPase activity was 0.58 ± 0.09 U/mg proteins. Three days after irradiation, Na^+/K^+ -ATPase activity was reduced to 52.6% of basal level. The Na^+/K^+ -ATPase activity measured in the irradiated and MSC-treated group was 0.66 ± 0.13 U/mg protein. Radiation-induced reduction of Na^+/K^+ -ATPase activity is thus reversed by MSC treatment, but not by fibroblasts infusion.

These results show for the first time an ability of hMSC to restore small intestinal function in a context of radiation-induced disorders.

Structural studies. We used morphometric analysis to evaluate the thickness of the small intestinal epithelium, which is a criterion for structural integrity. The estimated jejunum epithelium thickness in the control group was $320.6 \pm 11.8 \mu\text{m}$, obtained by adding the values of villus height ($244.0 \pm 9.0 \mu\text{m}$, functional cell compartment) to Lieberkühn crypt depth ($76.6 \pm 5.0 \mu\text{m}$, stem cell compartment) (Figure 3Aa and B). Twenty-four hours after irradiation, at the time of hMSC injection, no modification of the structural integrity of the small intestine was observed (data not shown). At 3 days, irradiation induced partial epithelial atrophy, corresponding to a reduction of 27% of villus height (Figure 3Ab and B). Irradiation-induced epithelial atrophy was not anymore observed at 15 days (data not shown). After MSC infusion into irradiated mice, the structural integrity of the small intestine was already

restored at 3 days (Figure 3Ac). The epithelium thickness measurement showed hypertrophy (increase of 69% versus control) resulting from increases in both crypt depth (167%) and villus height (38%, Figure 3B). The infusion of fibroblasts into irradiated mice did not restore structural integrity 3 days after irradiation. On the contrary, after fibroblast injection we observed ulcerated areas concomitant with inflammatory infiltration (Figure 3Ad). Owing to fibroblasts-induced pernicious effects on the epithelial structure, no quantitative measurement could be performed. These results showed that specifically hMSC treatment increases and accelerates the structural re-epithelization of the small intestine exposed to radiation.

The level of the epithelium hypertrophy observed into irradiated mice receiving hMSC treatment (Figure 3Ba) progressively decreased over time. At 120 days, epithelium thickness returned to the baseline level (Figure 4).

Cellular mechanisms of hMSC action. To study cellular mechanisms of hMSC action, the quantification and localization of epithelial apoptosis and proliferating cells were investigated. Cell positions were determined according to the methods established by Potten.³ Intermingled cells of Paneth cells, recently described by Clevers as intestinal stem cells, were also scored.¹¹ Characterization of intestinal stem cells was completed by an immunohistochemical analysis using Musashi-1 staining.

Apoptosis analysis. Apoptotic cells were studied on histological slides of small intestine by TUNEL assay (Figure 5A). We first analyzed the percentage of TUNEL-positive crypt–villus axis of a small intestine segment (Figure 5Ba). Second, for each TUNEL-positive crypt–villus axis, we determined the number of apoptotic cells in crypt compartments (Figure 5Bb) and the percentage of apoptotic cells in each cell category of the crypt–villus axis (Figure 5Bc).

Twenty-four hours after irradiation (time of hMSC infusion) we observed a five-fold increase in apoptotic epithelial cells in the small intestine. At this time, apoptotic cells were preferentially observed in positions 4–6 of crypts and between Paneth cells suggesting a stem and/or progenitor cell apoptosis (data not shown). Three days after irradiation, we still observed an induction of apoptosis (Figure 5Ab), detecting TUNEL-positive cells in $87.7 \pm 2.4\%$ of the crypt–villus axis, compared with $22.2 \pm 1.1\%$ in the control group (Figure 5Ba). Hence, we observed a dramatic 8.6-fold increase in apoptotic cells in crypt cell compartments exposed to radiation. Apoptotic cells were seen to be preferentially ($57.4 \pm 2.1\%$) located in positions 4–6 of crypts, likely corresponding to stem/progenitor cell apoptosis (Figure 5Bb and Bc). We also showed, after irradiation, an absence of apoptotic cells at the villi tip (Figure 5Bc), probably corresponding to the early stages of a reduction in the detachment-induced apoptosis of enterocytes (anoikis). These results seem to show that the self-renewal capability of the small intestine is significantly reduced after irradiation. hMSC infusion into irradiated mice (3 days) decreased (reduction of 51.3% versus irradiated animals) the percentage of crypt–villus axis containing apoptotic cells (Figure 5Ac and Ba). Furthermore, in irradiated mice treated with hMSC, the

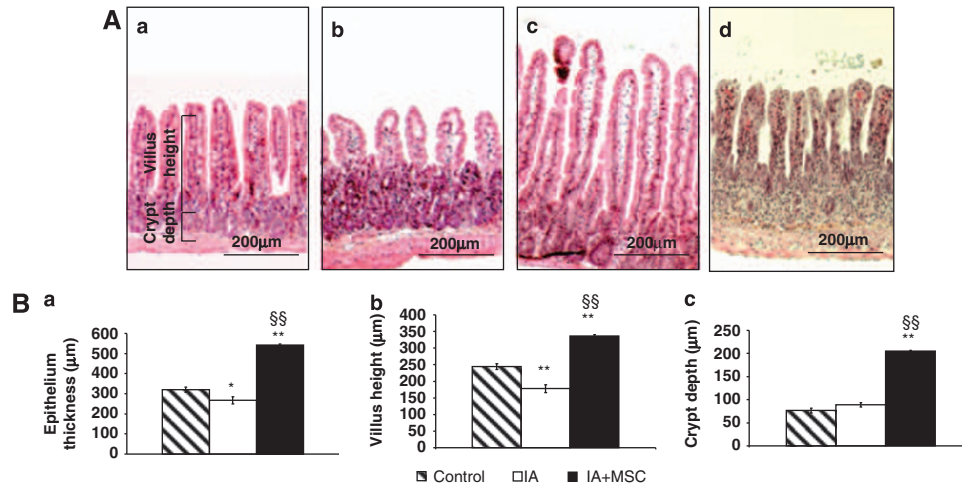


Figure 3 Human bone marrow-derived mesenchymal stem cell (hMSC) infusion restores small intestinal structure 3 days after irradiation (8.5 Gy). **(A)** Histological analysis: sections were stained with hematoxylin, eosin and safran (HES). Sections show: (a) control, (b) irradiated animals (IA), (c) irradiated animals receiving hMSC injection (IA + MSC) and (d) irradiated animals receiving human skin fibroblast injection (IA + F). Original magnification $\times 100$. Scale bars $200 \mu\text{m}$. **(B)** Quantitative analysis: measurements of (a) epithelium thickness (μm), (b) villus height (μm), and (c) crypt depth (μm). Each value represents the average of 20–30 independent measurements per animal (six animals per group) and shown for independently repeated experiments ($N=2$). Error bars represent S.E.M. $**P \leq 0.001$ versus control, $*P \leq 0.05$ versus control, $§§P \leq 0.001$ versus IA

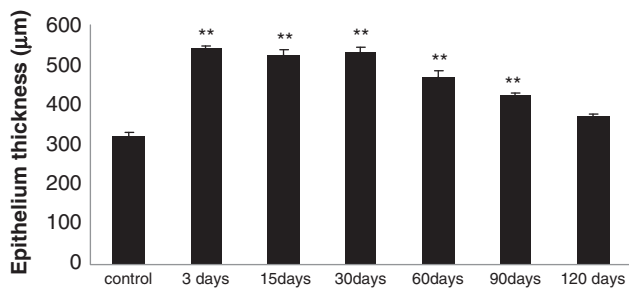


Figure 4 Time-dependent reduction of human bone marrow-derived mesenchymal stem cell (hMSC)-induced hypertrophy of small intestinal epithelium. Histogram shows a quantitative analysis of epithelium thickness (μm) of irradiated animals (8.5 Gy) receiving human MSC injection. Each value represents the average of 20–30 independent measurements per animal (six animals per group) and shown for independently repeated experiments ($N=2$). Error bars represent S.E.M. $**P \leq 0.001$ versus control

number of apoptotic cells in the crypt compartment returned to values close to the baseline (Figure 5Bb), corresponding to a specific decrease in the apoptosis of small intestinal stem/progenitor cells (Figure 5Bc). The percentage of apoptotic cells at the tip of villi observed after irradiation increased to $16.3 \pm 0.2\%$ after hMSC treatment, without reaching control values (Figure 5Bc). Fifteen days after irradiation and hMSC infusion, the number of apoptotic cells in crypt compartments fell back to control values (data not shown). We have hypothesized that the re-establishment of the self-renewal ability of small intestine after irradiation requires a decrease in apoptosis. We show that the hMSC treatment is associated with such a decrease.

Crypt cell proliferation. The number of proliferating crypt cells was assessed on histological slides of small intestine stained by Ki67 antibody (Figure 6A). The estimated basal

proliferation index (number of Ki67-positive cells per five crypts) was 46.0 ± 2.9 in the control group (Figure 6Aa and B). At the time of hMSC injection (24 h after irradiation) we observed a 21.5% reduction in the level of proliferating crypt cells, falling to 36.1 ± 1.5 (data not shown). At 3 days, we observed a 2.8-fold increase in proliferating crypt cells (Figure 6Ab and B). The percentage of proliferating cells increased in potential stem/progenitor cells located in positions 4–6 of crypts (increase of 37.2%), in dividing transit cells (increase of 6.8%) and in functional cells of crypt compartment (increase of 84.8%). We also observed a reduction in the percentage of potential stem cells intermingled with Paneth cells (reduction of 31.3%, Figure 6Bb). These results suggest that, 3 days after irradiation, the initiation of the small intestinal healing process seems to be under way. After hMSC infusion into irradiated mice, the crypt cell proliferation index peaks at a value of 206.3 ± 9.9 (increase of 61.0% versus irradiated animals, Figure 6Ac and Ba). We showed that hMSC treatment into irradiated mice reduced the loss of potential stem cells intermingled with the Paneth cells (decrease of 10.5% versus irradiated animals, Figure 6Bb). hMSC treatment also increased the percentage of proliferating cells in compartments that usually contain functional cells, that is cells of crypts in positions 15–20 (increase of 7.2% versus irradiated animals and 92.0% versus control animals) and cells of villi (increase of 10.2% versus irradiated animals and 12.0% versus control animals). Associated with the reduction in apoptosis, hMSC treatment also increases the proliferation of epithelial cells in the small intestine. Our results provide evidences that hMSC infusion into irradiated mice improves the self-renewal ability of small intestine and hence its restoration.

Immunostaining of small intestinal stem cells. In control group, Musashi-1 immunostaining was preferentially detected in intermingled cells of Paneth cells but also in

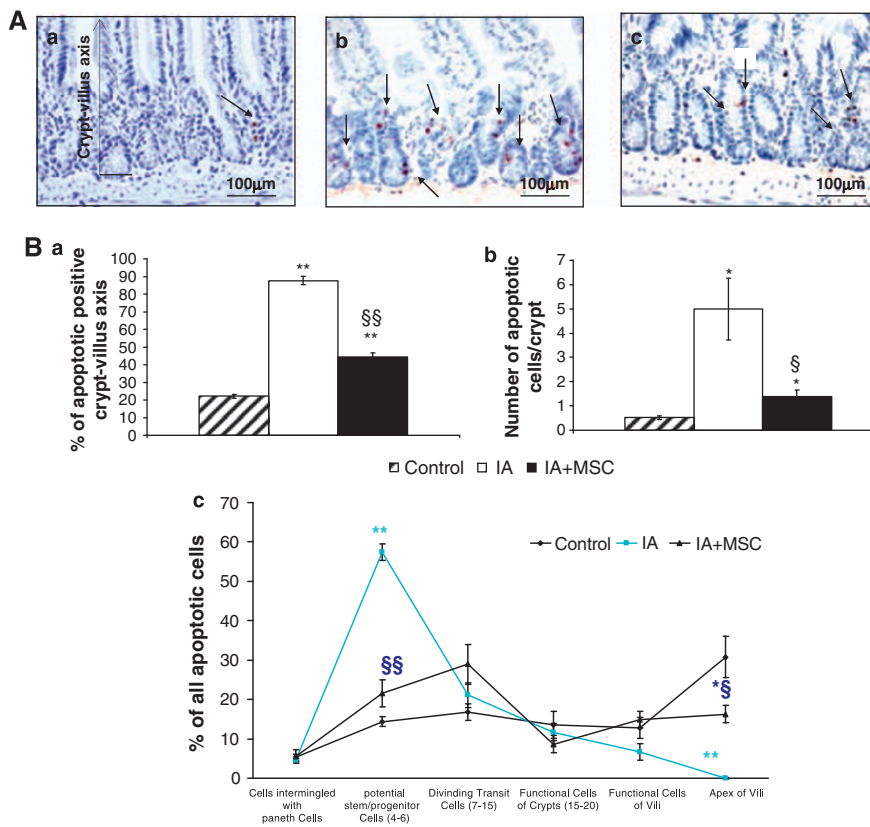


Figure 5 Human bone marrow-derived mesenchymal stem cell (hMSC) infusion reduces epithelial cell apoptosis induced 3 days after irradiation (8.5 Gy) in the small intestine. **(A)** Histological analysis: sections were stained by TUNEL assay and hematoxylin counterstained. Sections show (a) control, (b) irradiated animals (IA), (c) irradiated animals receiving hMSC injection (IA + MSC). Original magnification $\times 200$, scale bars $100 \mu\text{m}$. Black arrows show apoptotic cells. **(B)** Quantitative analysis: (a) percentage of apoptotic-positive crypt–villus axis, (b) number of apoptotic cells per crypt of each TUNEL-positive crypt–villus axis and (c) percentage of all apoptotic cells in each cell category of each TUNEL-positive crypt–villus axis. Each histogram value represents the average of 50 independent measurements of crypt–villus axis per animal (six animals per group) and shown for independently repeated experiments ($N = 2$). Error bars represent S.E.M. ** $P \leq 0.001$ versus control, * $P \leq 0.05$ versus control, §§ $P \leq 0.001$ versus IA, § $P \leq 0.05$ versus IA (pale blue: significative for IA group; dark blue: significative for IA + MSC group)

smaller proportion in position 4+ of crypts (Figure 6Ad). Three days after radiation exposure, Musashi-1 staining decreased considerably and became almost undetectable (Figure 6Ae). After hMSC treatment into irradiated mice, Musashi-1 immunoreactivity was detected in equal proportion in intermingled cells of Paneth cells and in position 4+ of crypts. Nevertheless, Musashi-1 detection was weaker in comparison with control group (Figure 6Af). Labeling of successive small intestinal sections with, respectively, Musashi-1 and Ki67 antibodies indicates that Musashi-1-positive cells have a high activity of cell proliferation (Figure 6Ag,h).

Human MSC infusion extends life of mice with radiation-induced severe gastrointestinal disorders. The therapeutic potential of hMSC was then analyzed in a model of severe and irreversible gastrointestinal disorders leading to death. Mice were subjected to a lethal dose of abdominal irradiation (10.5 Gy). As previously, a total of 5×10^6 cells was infused in the lateral tail vein of mice 24 h after irradiation. The therapeutic benefit and cellular mechanisms of hMSC treatment on radiation-induced death were analyzed.

Survival curve. We have shown that death occurs after 4–5 days in 100% of mice subjected to abdominal irradiation at a 10.5 Gy dose. Figure 7 shows that a treatment with hMSC delays radiation-induced death compared with vehicle ($P < 0.034$).

Structural studies. Death of the animals occurring 5 days after irradiation (10.5 Gy) was associated with significant ulceration of the small intestinal epithelium, corresponding to $80.0 \pm 15\%$ of the epithelium surface (SEU) (Figure 8Aa and Ab). The infusion of hMSC into irradiated animals induced a non-significant ($P = 0.4$) reduction of the ulcerated epithelium surface, falling to $62 \pm 15\%$ (Figure 8Ac).

Cellular effects of hMSC infusion. Analyses were done on the margin of epithelial ulceration. After hMSC treatment, we observed a 2.5-fold reduction of radiation-induced apoptotic cells in crypt cell compartments (Figure 8Ba). At this time, the infusion of hMSC into irradiated animals enhanced the number of crypt cells in proliferation (increase of 109.9% versus control, Figure 8Bb).

Hence, 5 days after radiation-induced irreversible gastrointestinal tract (GIT) lesions, the small intestinal epithelium on

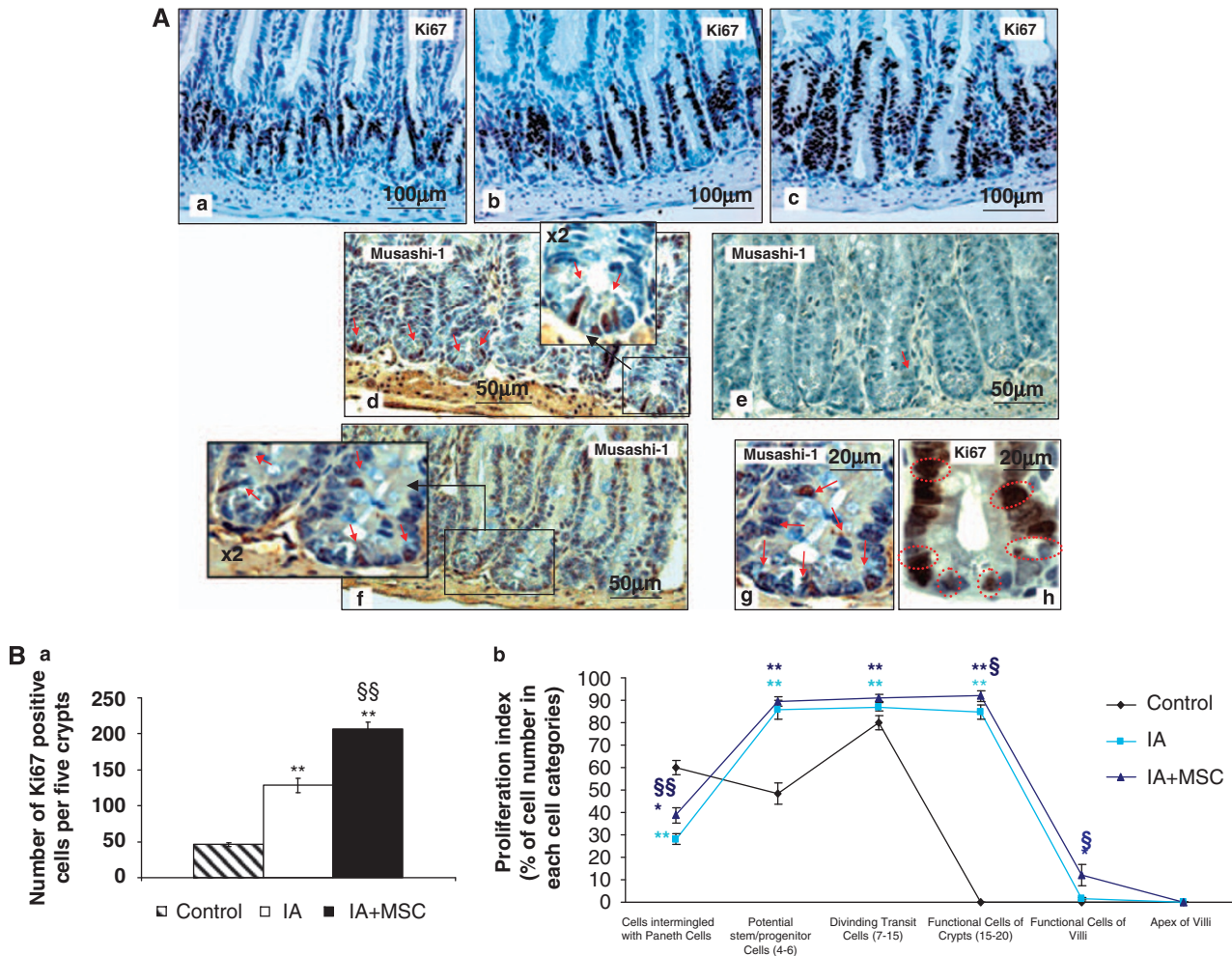


Figure 6 Human bone marrow-derived mesenchymal stem cell (hMSC) infusion increases epithelial cell proliferation of the small intestine 3 days after irradiation (8.5 Gy). **(A)** Histological analysis: sections show: (a, d) control, (b, e) irradiated animals (IA), (c, f-h) irradiated animals receiving hMSC injection (IA + MSC). Sections (a-c) and (h) were stained in black/dark brown by Ki67 antibody. Sections (d-g) were stained in dark brown by Musashi-1 antibody (red arrows). Sections (g) and (h) represent successive sections and show the same crypt stained either by Musashi-1 or by Ki67 antibodies. Musashi-1-positive cells (g) are also positive for Ki67 (h, circles in red dotted line). All sections were hematoxylin counterstained. Original magnification, $\times 200$, $\times 453$ and $\times 931$ corresponding to scale bars 100, 50 and 20 μm , respectively. **(B)** Quantitative analysis: (a) number of Ki67-positive cells per five crypts, (b) percentage of Ki67-positive cells in each cell category of each crypt-villus axis. Each value represents the average of 50 independent measurements per animal (six animals per group) and shown for independently repeated experiments ($N=2$). Error bars represent S.E.M. $**P \leq 0.001$ versus control, $*P \leq 0.05$ versus control, $§§P \leq 0.001$ versus IA, $§P \leq 0.05$ versus IA (pale blue: significant for IA group; dark blue: significant for IA + MSC group)

the margin of ulcerated areas keeps the properties of renewal when hMSC are administered.

Discussion

Our results reveal a therapeutic benefit of MSC treatment on radiation-induced gastrointestinal disorders. As described earlier, we reported that radiation-induced epithelial dysfunctions account for partial mucosal atrophy resulting from stem/progenitor cell depletion, and therefore a subsequent impairment of epithelial self-renewal.³ We showed that MSC treatment (1) increases and accelerates the recovery of the small intestine with reversible alterations and (2) extends the life of animals developing irreversible gastrointestinal alterations. Histological evaluations provided initial insight into the cellular targets of therapy. MSC effects are a consequence of

their ability to enhance or maintain the re-epithelization process of small intestinal epithelium. To our knowledge, this is the first demonstration that MSC therapeutic effects on small intestinal damage lead to the re-establishment of cellular homeostasis by both increasing endogenous proliferation processes and inhibiting apoptosis of radiation-induced intestinal epithelial cells.

Our study shows an ability of MSC to accelerate structural restoration (re-epithelization process) of the small intestine, thus improving functional rescue. We report here the ability of MSC to bring about fast recovery of radiation-induced dysfunctions of the secretory response of small intestinal epithelium (electrolyte and water transport, that is chloride secretion across epithelial cells). Stringent physiological regulation of chloride secretion, and thus also water secretion, into the lumen of intestine prevents or reduces the

trans-epithelial migration of bacteria, bacterial products or antigens into the lamina propria, which could trigger an inappropriate and potentially chronic inflammatory response.¹²

We also showed MSC abilities to restore radiation-induced dysfunctions of the absorptive response of small intestinal epithelium (membrane Na^+/K^+ -ATPase activity of epithelial cells). The activity of the Na^+/K^+ -ATPase pump maintains

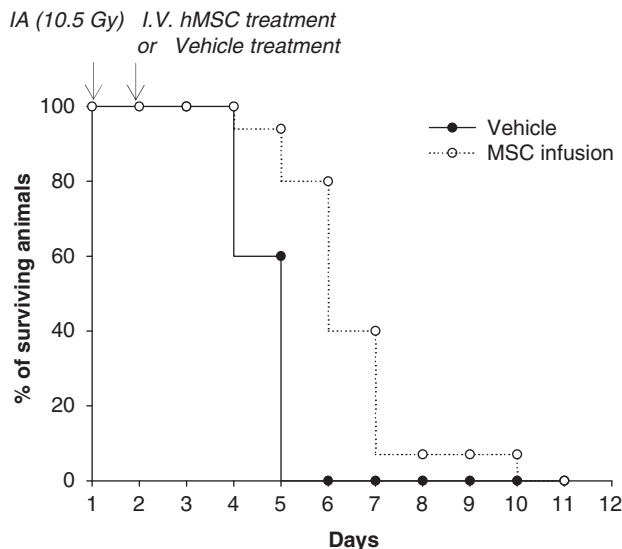


Figure 7 Human bone marrow-derived mesenchymal stem cell (hMSC) injection extends life in an animal model of radiation-induced severe gastrointestinal disorders: NOD/SCID mice were subjected to lethal abdominal irradiation at a 10.5 Gy dose. hMSC were administered by intravenous infusion. Controls received vehicle. Time points of interventions are given above survival plots. Results are cumulative data of two independent experiments ($n=20$ for vehicle and $n=15$ for MSC infusion) using different batches of hMSC. P -value determined by log-rank test

Na^+ , K^+ and membrane potential gradient across the enterocyte membrane, which are driving forces for transporting most amino acids and/or sugars.¹³ Na^+/K^+ -ATPase activity provides the electrochemical gradient that subsequently increases the driving force for chloride efflux from epithelial cells across the apical membrane.¹³ MSC-induced re-establishment of membrane Na^+/K^+ -ATPase activity of small intestinal epithelial cells might be a precursor of chloride-secretion restoration and/or could even maximize it. These two functional rescues induced by MSC infusion involve the re-establishment of an ionic gradient across the epithelial membrane. To our knowledge, there are no reports in the literature of such an *in vivo* ionic flux regulation by MSC in the GIT. Some *in vivo* electrophysiological experiments have revealed the capacity of MSC to increase conduction velocity (reduction of conduction latency and enhancement of action potential number and amplitude) of motor nerves¹⁴ and somatosensory nerves¹⁵ for functional recovery of injured peripheral nervous system. Moreover, an *in vitro* study has shown that MSC are able to repair cross-channel electrical conduction blocking in cardiomyocytes.¹⁶

Earlier authors have found evidence of trans-differentiation in the intestine after cell therapy after infusion of total BM cells. BM-derived cells could reside in the small intestine as late transit cells with limited dividing potential¹⁷ and, after injury, could in turn form specific epithelial cell lineages for organ restoration.¹⁸

In our study, the small number of human-derived cells implanted into the intestinal mucosa means that the replacement of epithelial cell loss by trans-differentiation is unlikely to represent the main therapeutic principle. Nevertheless, we reported that MSC are able to restore small intestinal integrity by maintaining cellular and tissue homeostasis, through the specific regulation of epithelial cells. MSC treatment produces

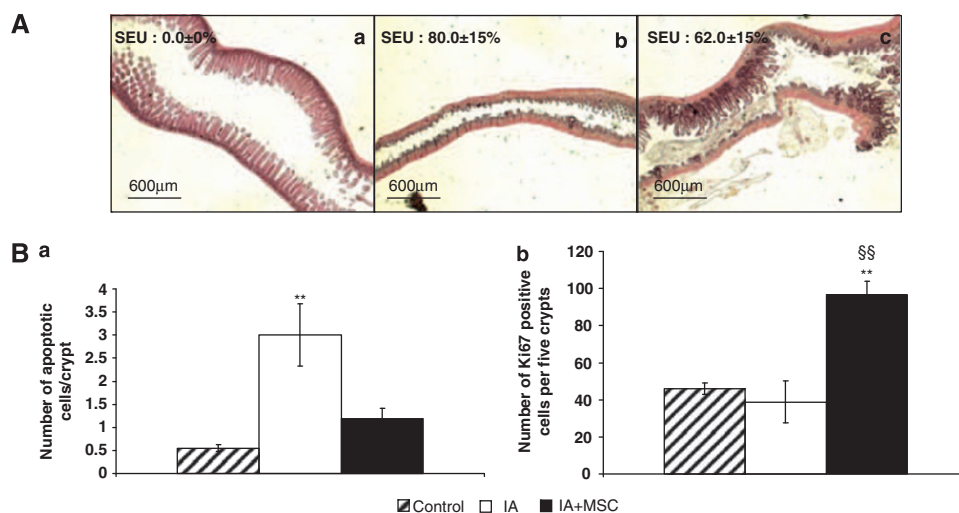


Figure 8 (A) Human bone marrow-derived mesenchymal stem cell (hMSC) effects after radiation-induced irreversible gastrointestinal disorders. Histological analysis: sections were stained with hematoxylin, eosin and safran (HES). Sections show: (a) control, (b) irradiated animals (IA), (c) irradiated animals receiving hMSC injection (IA + MSC). Original magnification $\times 56.4$, scale bars $600 \mu\text{m}$. SEU is the surface of epithelium ulceration per sections. Each value represents the average of the measurement of five sections per animal (six to eight animals per group) (B) Quantitative analysis on the margin of epithelium ulceration: (a) number of apoptotic cells per crypt, (b) number of Ki67-positive cells per five crypts. Each value represents the average of 30–50 independent measurements per animal (six to eight animals per group). Error bars represent S.E.M. $**P \leq 0.001$ versus control, $^{SS}P \leq 0.001$ versus IA

an enhancement of radiation-induced epithelial crypt cell proliferation and reduces radiation-induced epithelial apoptosis in the intestine. The contribution of MSC to increasing proliferation and/or reducing apoptosis for organ rescue has been broadly shown *in vivo* for renal epithelial cells¹⁹ and nerve cells²⁰ as a therapeutic benefit. Moreover, some results obtained *in vitro* show similar effects of MSC on the regulation of apoptosis and/or proliferation of renal epithelial cells,²¹ endothelial cells such as aortic cells,²² brain microvascular cells²³ and cardiomyocytes.²⁴ Finally, convincing *in vitro* results obtained by Parekkadan *et al.*²⁵ show, on the contrary, that MSC favor the death and reduce the proliferation of resident liver cells, specifically activated stellate cells. In the latter case, by limiting the activation of liver stellate cells, the authors suggest that MSC also have a therapeutic effect by preventing fibrosis. Our results seem to show that after radiation exposure, MSC treatment could maintain some active intestinal stem cells with ability of proliferation. Clevers and co-workers²⁶ showed that a single intestinal stem cell can operate independently of positional cues from its environment and that it can generate a continuously expanding, self-organizing epithelial structure, reminiscent of normal intestine. Hence, the partial rescue of intestinal stem cell level induced by MSC treatment could be sufficient to induce recovery of small intestinal integrity.

MSC might regulate the epithelial stem/progenitor cells directly or indirectly, that is stem cell niches that provide and maintain an optimal microenvironment for stem cell function. Several studies seem to support this hypothesis of secondary stem cell niche replenishment or restoration. First, MSC has already been described as maintaining stem cell niches, for example in BM.²⁷ Second, BM-derived cells can be traced into the pericryptal and lamina propria meshwork (as sometimes observed in these experiments), giving rise to mesenchymal lineages that regulate epithelial cell proliferation and differentiation through mesenchymal–epithelial paracrine interactions.²⁸ Recent studies have documented hMSC synthesis and release of several cytokines and growth factors such as, for instance, IL-11, HGF, FGF-2 and IGF-I.^{29–31} Each of these factors has been described earlier as facilitating intestinal mucosa repair, either through enhancement of cell proliferation or inhibition of epithelial cell apoptosis, or by a combination of both.^{32–35} The therapeutic benefit of MSC reported in this study could be the consequence of releases and synergic effects of multiple paracrine factors. Further research is needed to elucidate this complex issue.

After MSC therapy, we report re-establishment of structural and cellular homeostasis over time. We can therefore exclude any subsequent running of out of control of MSC as affecting the regulation of small intestinal epithelium.

Conclusion

This study provides evidence for the potential of MSC to limit radiation effects on the small intestine. MSC actions involve cellular homeostasis stabilization, which arises from the regulation and preservation of endogenous epithelial cells. The rescue of epithelial cell integrity by MSC after abdominal or pelvic radiotherapy might favor renewal of healthy intestinal

tissue. This might reduce acute and/or chronic side effects and may be of therapeutic interest.

Materials and Methods

All experiments and procedures were performed in accordance with the French Ministry of Agriculture regulations for animal experimentation (Act no. 87–847 of 19 October 1987, amended May 2001) and were approved by the animal care committee of the Institut de Radioprotection et de Sécurité Nucléaire (IRSN). Male NOD-LtSz-*scid/scid* (NOD-SCID) mice (20–25 g, 10-weeks old), from breeding pairs originally purchased from Jackson Laboratory (Bar Harbor, ME, USA), were bred in our pathogen-free unit and maintained in sterile micro-isolator cages.

Small intestinal integrity analysis. Small intestinal integrity analysis was performed on samples harvested from NOD/SCID mice subjected to a sub-lethal dose of irradiation. Mice received total body irradiation (TBI) at a dose of 3.5 Gy immediately followed by local irradiation to the abdomen at a dose of 5 Gy for a total dose of 8.5 Gy to the abdominal region. Animals were killed 3, 15, 30, 60, 90, 120 days after irradiation and small intestine (jejunum) was collected for functional, structural and cellular homeostasis analysis.

Survival curve analysis. NOD/SCID mice were subjected to a lethal dose of irradiation. Mice received TBI at a dose of 3.5 Gy immediately followed by local irradiation to the abdomen at a dose of 7 Gy for a total dose of 10.5 Gy to the abdominal region. Animal survival was monitored every 12 h. In these experiments, some animals were reserved to analyze structural and cellular homeostasis 5 days after radiation exposure.

Preparation and delivery of hMSC. BM cells were obtained after informed consent of patients undergoing total hip replacement surgery and were used in accordance with the procedures approved by the human experimentation and ethics committees of Hospital St-Antoine (France). BM of 10–20 ml were harvested in α -MEM (Invitrogen, Cergy, France) supplemented with heparin. Total cells were isolated from bone fragments. Nucleated cells were plated at 50 000 cells/cm² in α -MEM supplemented with 10% fetal calf serum (research grade FCS, Hyclone, Perbio, France), 1% L-glutamine, 1% penicillin streptomycin and 1 ng/ml β FGF (Sigma-Aldrich Chimie SARL, Lyon, France) as used in clinics.⁶ Culture flasks were incubated at 37°C with 5% CO₂ in a humidified atmosphere. After 72 h, non-adherent cells were removed, and the medium was replaced twice a week until the 90% confluence was reached. Samples of hMSC from different donors were collected at passage 2 for transplantation. A total of 5×10^6 cells was infused in the lateral tail vein 24 h after irradiation. At the time of infusion, hMSC were characterized by the expression of CD73 (SH3) and CD105 (SH2) and the lack of expression of CD45 using FACS analysis³⁶ and by their potential for osteogenic and adipogenic differentiation.³⁷ The specificity of hMSC effects was tested by the infusion of 5×10^6 human skin fibroblasts (institute self-production) in the lateral tail vein 24 h after irradiation.

Functional analyses

Ussing chamber experiments. Tissue samples were rinsed with ice-cold saline (0.9% NaCl) and opened longitudinally along the mesenteric border. Tissues were mounted in Ussing chambers with 0.126 cm² apertures (1/2 chamber volume: 5 ml, Corning Costar Corporation, Cambridge, MA, USA). Tissues were bathed with a modified Krebs buffer containing (in mM) 115.0 NaCl, 8.0 KCl, 2.0 KH₂PO₄, 2.4 MgCl₂, 1.3 CaCl₂, 25.0 NaHCO₃, pH 7.4, at 37°C and gassed with 95% O₂/5% CO₂. The serosal buffer contained 10.0 mM glucose, whereas the mucosal buffer contained 10.0 mM mannitol to avoid mucosal active sodium/glucose co-transport. Tissue responses to EFS were measured by clamping the potential difference at 0 mV, under short-circuit current (*I*_{sc}) conditions with a voltage-clamp apparatus (DVC-1000, World Precision Instruments, Hertfordshire, UK). After a 15 min equilibration period, *I*_{sc} was recorded continuously as the indicator of net active electrolyte transport across the tissue. EFS (100 V, pulse duration 500 μ s, total stimulation time 3 s, frequency 5 Hz) was applied with a dual impedance stimulator (Harvard Instruments, Ealing, Les Ulis, France).

Enzyme activity. Na⁺/K⁺-ATPase activity was estimated using an ouabain-sensitive, K⁺-stimulated *p*-nitrophenyl phosphatase assay.³⁸ Results were expressed per milligram (mg) of protein, estimated using the dye-binding method of Bradford³⁹ with bovine serum albumin (BSA).

Histology methods. Formalin-fixed, paraffin-embedded small intestines were cut at 5 μm on a rotary microtome (Leica Microsystems AG, Wetzlar, Germany) and mounted on polysine slides. Sections were deparaffinized in xylene and rehydrated through ethanol baths and PBS.

Hydrated sections were stained with hematoxylin, eosin and safran. The sections were studied for histological changes in the mucosa. The epithelium thickness was measured in μm using image analysis software (Visiolab, Biocom, France).

β -2-microglobulin staining. Endogenous enzymes were blocked using 3% H_2O_2 in methanol for 10 min. Tissue sections were rinsed with 1:10 diluted TBST (Dakocytomation, Dako France S.A.S, Trappes, France, S3306) for 5 min. To expose masked epitopes, tissue sections were digested with 2% trypsin for 10 min at 37°C in a humidified chamber. Sections were washed in 1:10 diluted TBST (Dakocytomation, S3306) and incubated with serum-free protein block (Dakocytomation, X0909). Polyclonal rabbit anti-human β -2-microglobulin antibody (product NCL-B2Mp, Novocastra, A Menarini Diagnostics, Rungis, France) was then added at a dilution of 1:1000. Slices were incubated in primary antibody for 60 min and rinsed twice in 1:10 diluted TBST (Dakocytomation, S3306). The rabbit envision + HRP system and Vector Novared substrate (Vector Laboratories, Burlingame, CA, USA) were used to produce visible results. Sections were lightly counterstained with Mayer's hemalum solution (Merck Chimie S.A.S, Fontenay-sous-Bois, France).

TUNEL staining. Hydrated sections were incubated with 20 $\mu\text{g}/\text{ml}$ proteinase K (Roche Diagnostic, Meylan, France) for 10 min at 37°C. Slices were washed with PBS and the endogenous peroxidases were quenched with 3% H_2O_2 in methanol for 10 min at room temperature. Slices were washed in PBS and incubated with serum-free protein block (Dakocytomation, X0909). Sections were incubated with TdT labeling reaction using *in situ* cell death detection, POD, (Roche Diagnostic) according to the manufacturer. After washing, color development was achieved using Vector Novared substrate (Vector Laboratories). Tissues were counterstained with Mayer's hemalum solution (Merck, Germany).

Ki67 staining. Hydrated sections were dipped into permeabilization solution consisting of 0.1% Triton X-100 in PBS and were rinsed in a distilled water bath for 5 min. To expose masked epitopes, tissues were incubated for 30 min in 10 mmol/l buffered citrate, pH 6.0. After washing in distilled water, endogenous enzymes were blocked using 3% hydrogen peroxide (H_2O_2) in methanol for 10 min and washed again in a 50 mM Tris buffer containing 9 g/l NaCl (TBS). Non-specific antibody binding was minimizing by incubating sections overnight at 4°C in 50 mmol/l Tris buffer containing 4% BSA. Endogenous avidins and peroxidases were inhibited, respectively, using Blocker A and Blocker B (Ventana Medical Systems SA, Illkirch, France) for 10 min followed by 5 min wash in TBS. Tissues were incubated in the presence of the primary antibody, Ki67 monoclonal rat anti-mouse antibody (Dakocytomation, M7249), at a dilution of 1:100 in 1% BSA, 50 mmol/l Tris buffer solution for 60 min at 37°C in a humidified chamber. Sections were rinsed in TTC buffer consisting of 50 mmol/l Tris, 0.05% Tween-20 (Sigma) and 0.6 g/l casein (Sigma). Bound primary antibody was detected with biotinylated rabbit anti-rat IgG secondary antibody (Dakocytomation, E0468). The secondary antibody was diluted 1:200 in 1% BSA, 50 mmol/l Tris buffer solution and incubated for 60 min at 37°C in a humidified chamber. Sections were rinsed in TTC. The ABC-HRP and Vector Novared substrate (Vector Laboratories) were used to produce visible results. Sections were lightly counterstained with Mayer's hemalum solution (Merck, Germany).

Apoptotic and proliferating cells were determined using image analysis software (Visiolab).

Musashi-1 staining. Hydrated sections were dipped into permeabilization solution consisting of 0.2% Triton X-100 in PBS 1 \times and blocked with 3% BSA in PBS 1 \times , 60 min at room temperature. After washing in PBS (three times), primary antibody rat monoclonal anti-Musashi-1 (14H1) kindly supplied by Professor Hideyuki Okano was then applied overnight at 4°C at a dilution of 1:100. Section were three times washed in PBS 1 \times . Bound primary antibody was detected with (1:300) biotinylated polyclonal rabbit anti-rat IgG secondary antibody (Dakocytomation, E0467) incubated 30 min at room temperature. After washing in PBS 1 \times , the ABC-HRP (Dakocytomation, K0377) and Vector Novared substrate (Vector Laboratories) were used to produce visible results. Sections were lightly counterstained with Mayer's hemalum solution (Merck, Germany).

Statistical analysis. Data are given as mean \pm S.E.M. (standard error of the mean). Results were compared between groups by a *t*-test or a one-way ANOVA followed by a Tukey test using Sigmastat software (Systat Software Incorporation, GmbH, Erkrath, Germany). Significance for analyses was set at $**P \leq 0.001$ versus

control, $*P \leq 0.05$ versus control, $^{**}P \leq 0.001$ versus IA, $^{\$}P \leq 0.05$ versus IA. Mouse survival curves were calculated by Kaplan-Meier method and *P*-value was determined by log-rank test.

Conflict of interest

The authors declare no conflict of interest.

Acknowledgements. We are grateful to Dr. Pouzoulet Frédérique who produced human skin fibroblasts. We are indebted to Professor Hideyuki Okano who kindly supplied us with anti-Musashi-1 14H-1 antibody and for his assistance for immunohistochemistry. This work was supported by grants from EDF (Electricité de France) and EEC (FIRST: contract number 503436).

- Denham JW, Hauer-Jensen M. The radiotherapeutic injury—a complex 'wound'. *Radiation Oncol* 2002; **63**: 129–145.
- Erbil Y, Oztezcan S, Giris M, Barbaros U, Olgac V, Bilge H *et al*. The effect of glutamine on radiation-induced organ damage. *Life Sci* 2005; **78**: 376–382.
- Potten CS. Radiation, the ideal cytotoxic agent for studying the cell biology of tissues such as the small intestine. *Radiat Res* 2004; **161**: 123–136.
- Francois A, Milliat F, Vozenin-bretons M. Bowel injury associated with pelvic radiotherapy. *Radiat Phys Chem* 2005; **72**: 399–407.
- Ash D. Lessons from epinal. *Clin Oncol (R Coll Radiol)* 2007; **19**: 614–615.
- Fouillard L, Bensedhoum M, Bories D, Bonte H, Lopez M, Moseley AM *et al*. Engraftment of allogeneic mesenchymal stem cells in the bone marrow of a patient with severe idiopathic aplastic anemia improves stroma. *Leukemia* 2003; **17**: 474–476.
- Horwitz EM, Gordon PL, Koo WK, Marx JC, Neel MD, McNall RY *et al*. Isolated allogeneic bone marrow-derived mesenchymal cells engraft and stimulate growth in children with osteogenesis imperfecta: implications for cell therapy of bone. *Proc Natl Acad Sci USA* 2002; **99**: 8932–8937.
- Le Blanc K, Rasmusson I, Sundberg B, Gotherstrom C, Hassan M, Uzunel M *et al*. Treatment of severe acute graft-versus-host disease with third party haploidentical mesenchymal stem cells. *Lancet* 2004; **363**: 1439–1441.
- Ringden O, Uzunel M, Sundberg B, Lonnie L, Nava S, Gustafsson J *et al*. Tissue repair using allogeneic mesenchymal stem cells for hemorrhagic cystitis, pneumomediastinum and perforated colon. *Leukemia* 2007; **21**: 2271–2276.
- Garcia-Olmo D, Garcia-Arraz M, Herreros D, Pascual I, Peiro C, Rodriguez-Montes JA. A phase I clinical trial of the treatment of Crohn's fistula by adipose mesenchymal stem cell transplantation. *Dis Colon Rectum* 2005; **48**: 1416–1423.
- Barker N, van Es JH, Kuipers J, Kujala P, van den Born M, Cozijnsen M *et al*. Identification of stem cells in small intestine and colon by marker gene Lgr5. *Nature* 2007; **449**: 1003–1007.
- Wood JD. Neuro-immunophysiology of colon function. *Pharmacology* 1993; **47**: 7–13.
- Schultz SG, Hudson RL. Biology of sodium-absorbing epithelial cells: dawning of a new era. In: Schultz SG, Field M, Frizzell RA, Rauner BB (eds). *Handbook of Physiology: The Gastrointestinal System*, vol. 4, Intestinal Absorption and Secretion. American Physiological Society: Bethesda, MA, USA, 1991, pp 45–81.
- Pan HC, Cheng FC, Chen CJ, Lai SZ, Lee CW, Yang DY *et al*. Post-injury regeneration in rat sciatic nerve facilitated by neurotrophic factors secreted by amniotic fluid mesenchymal stem cells. *J Clin Neurosci* 2007; **14**: 1089–1098.
- Lim JH, Byeon YE, Ryu HH, Jeong YH, Lee YW, Kim WH *et al*. Transplantation of canine umbilical cord blood-derived mesenchymal stem cells in experimentally induced spinal cord injured dogs. *J Vet Sci* 2007; **8**: 275–282.
- Beeres SL, Atsma DE, van der Laarse A, Pijnappels DA, van Tuyn J, Fibbe WE *et al*. Human adult bone marrow mesenchymal stem cells repair experimental conduction block in rat cardiomyocyte cultures. *J Am Coll Cardiol* 2005; **46**: 1943–1952.
- Marshman E, Booth C, Potten CS. The intestinal epithelial stem cell. *Bioessays* 2002; **24**: 91–98.
- Matsumoto T, Okamoto R, Yajima T, Mori T, Okamoto S, Ikeda Y *et al*. Increase of bone marrow-derived secretory lineage epithelial cells during regeneration in the human intestine. *Gastroenterology* 2005; **128**: 1851–1867.
- Togel F, Hu Z, Weiss K, Isaac J, Lange C, Westenfelder C. Administered mesenchymal stem cells protect against ischemic acute renal failure through differentiation-independent mechanisms. *Am J Physiol Renal Physiol* 2005; **289**: F31–F42.
- Chen J, Li Y, Katakowski M, Chen X, Wang L, Lu D *et al*. Intravenous bone marrow stromal cell therapy reduces apoptosis and promotes endogenous cell proliferation after stroke in female rat. *J Neurosci Res* 2003; **73**: 778–786.
- Imberti B, Morigi M, Tomasoni S, Rota C, Coma D, Longaretti L *et al*. Insulin-like growth factor-1 sustains stem cell mediated renal repair. *J Am Soc Nephrol* 2007; **18**: 2921–2928.
- Moon MH, Kim SY, Kim YJ, Kim SJ, Lee JB, Bae YC *et al*. Human adipose tissue-derived mesenchymal stem cells improve postnatal neovascularization in a mouse model of hindlimb ischemia. *Cell Physiol Biochem* 2006; **17**: 279–290.

23. Liu K, Chi L, Guo L, Liu X, Luo C, Zhang S *et al*. The interactions between brain microvascular endothelial cells and mesenchymal stem cells under hypoxic conditions. *Microvasc Res* 2008; **75**: 59–67.
24. Sadat S, Gehmert S, Song YH, Yen Y, Bai X, Gaiser S *et al*. The cardioprotective effect of mesenchymal stem cells is mediated by IGF-I and VEGF. *Biochem Biophys Res Commun* 2007; **363**: 674–679.
25. Parekkadan B, van Poll D, Megeed Z, Kobayashi N, Tilles AW, Berthiaume F *et al*. Immunomodulation of activated hepatic stellate cells by mesenchymal stem cells. *Biochem Biophys Res Commun* 2007; **363**: 247–252.
26. Sato T, Vries RG, Snippert HJ, van de Wetering M, Barker N, Stange DE *et al*. Single Lgr5 stem cells build crypt-villus structures *in vitro* without a mesenchymal niche. *Nature* 2009; **459**: 262–265.
27. Moore KA, Lemischka IR. Stem cells and their niches. *Science* 2006; **311**: 1880–1885.
28. Brittan M, Chance V, Elia G, Poulsom R, Alison MR, MacDonald TT *et al*. A regenerative role for bone marrow following experimental colitis: contribution to neovasculogenesis and myofibroblasts. *Gastroenterology* 2005; **128**: 1984–1995.
29. Crisostomo PR, Wang Y, Markel TA, Wang M, Lahm T, Meldrum DR. Human mesenchymal stem cells stimulated by Tnf, Lps, or hypoxia produce growth factors by an Nfkb but Not Jnk dependent mechanism. *Am J Physiol Cell Physiol* 2008; **294**: C675–C682.
30. Kim DH, Yoo KH, Choi KS, Choi J, Choi SY, Yang SE *et al*. Gene expression profile of cytokine and growth factor during differentiation of bone marrow-derived mesenchymal stem cell. *Cytokine* 2005; **31**: 119–126.
31. Schinkothe T, Bloch W, Schmidt A. *In vitro* secreting profile of human mesenchymal stem cells. *Stem Cells Dev* 2008; **17**: 199–206.
32. Boerma M, Wang J, Burnett AF, Santin AD, Roman JJ, Hauer-Jensen M. Local administration of interleukin-11 ameliorates intestinal radiation injury in rats. *Cancer Res* 2007; **67**: 9501–9506.
33. Houchen CW, George RJ, Sturmoski MA, Cohn SM. FGF-2 enhances intestinal stem cell survival and its expression is induced after radiation injury. *Am J Physiol* 1999; **276**: G249–G258.
34. Kanayama M, Takahara T, Yata Y, Xue F, Shinno E, Nonome K *et al*. Hepatocyte growth factor promotes colonic epithelial regeneration via Akt signaling. *Am J Physiol Gastrointest Liver Physiol* 2007; **293**: G230–G239.
35. Mylonas PG, Matsouka PT, Papandoniou EV, Vagianos C, Kalfarentzos F, Alexandrides TK. Growth hormone and insulin-like growth factor I protect intestinal cells from radiation induced apoptosis. *Mol Cell Endocrinol* 2000; **160**: 115–122.
36. Nasef A, Mathieu N, Chapel A, Frick J, Francois S, Mazurier C *et al*. Immunosuppressive effects of mesenchymal stem cells: involvement of HLA-G. *Transplantation* 2007; **84**: 231–237.
37. Mouiseddine M, Francois S, Semont A, Sache A, Allenet B, Mathieu N *et al*. Human mesenchymal stem cells home specifically to radiation-injured tissues in a non-obese diabetes/severe combined immunodeficiency mouse model. *Br J Radiol* 2007; **80**: S49–S55.
38. Murer H, Ammann E, Biber J, Hopfer U. The surface membrane of the small intestinal epithelium. I. Localization of adenylate cyclase. *Biochim Biophys Acta* 1979; **433**: 509–519.
39. Bradford MM. A rapid and sensitive method for the quantitation of microgram quantities of protein utilizing the principle of protein-dye binding. *Anal Biochem* 1976; **72**: 248–254.
40. Kaneko Y, Sakakibara S, Imai T, Suzuki A, Nakamura Y, Sawamoto K *et al*. Musashi1: an evolutionally conserved marker for CNS progenitor cells including neural stem cells. *Dev Neurosci* 2000; **22**: 139–153.